FULL PAPER

BJC

British Journal of Cancer (2017) 117, 1349–1359 | doi: 10.1038/bjc.2017.273

Keywords: DHX15; transposon mutagenesis; tumour suppressor gene; RNA helicase; glioma; glioblastoma

RNA helicase DHX15 acts as a tumour suppressor in glioma

Shingo Ito[1,2], Hideto Koso[1], Kazuhiro Sakamoto[2] and Sumiko Watanabe*[,1]

[1]Division of Molecular and Developmental Biology, Institute of Medical Science, University of Tokyo, Tokyo 1088639, Japan and [2]Department of Coloproctological Surgery, Faculty of Medicine, Juntendo University, Tokyo 1138421, Japan

Background: Glioblastoma is the most common form of malignant brain cancer and has a poor prognosis in adults. We identified *Dhx15* as a candidate tumour suppressor gene in glioma by transposon-based mutagenesis. *Dhx15* is an adenosine triphosphate (ATP)-dependent RNA helicase belonging to the DEAH-box (DHX) helicase family, but its role in cancer remains elusive.

Methods: DHX15 expression levels were examined in glioma cell lines. DHX15 functions were examined by gain- and loss-of-function analyses. Protein motifs required for the function of DHX15 were investigated by the analysis of mutant proteins.

Results: *DHX15* expression was lower in human glioma cell lines than in normal neural stem cells. *Dhx15* knockdown resulted in enhanced proliferation of primary immortalised mouse astrocytes, supporting the notion that DHX15 is a tumour suppressor. Retroviral-mediated transduction of *DHX15* into glioma cell lines suppressed proliferation and foci formation *in vitro*. Moreover, DHX15 suppressed tumour formation in a xenograft mouse model. ATPase activity was not required for the growth-inhibitory function of DHX15; however, the Ia, Ib, IV, and V motifs, which act as RNA-binding domains in DHX15, were essential. qPCR analysis revealed that DHX15 suppressed expression of NF-κB downstream target genes as well as the genes involved in splicing.

Conclusions: These findings provide evidence that DHX15 acts as a tumour suppressor gene in glioma.

Glioblastoma (GBM) is the rapid growth of a malignant primary brain tumour in adults. Patients with GBM have a poor prognosis and usually survive less than 15 months following diagnosis (Levin *et al*, 2001). Multimodality treatment with surgery, radiotherapy, or chemotherapy can improve patient survival, but an effective long-term treatment for this disease has not been established (Walid, 2008). Therefore, the development of novel treatment options is urgently needed. Recent genome re-sequencing studies have identified a large number of somatic mutations in GBM (Brennan *et al*, 2013); however, the roles of these mutations in the initiation and progression of glioma remain largely unknown. Transposon-based insertional mutagenesis provides an unbiased method for a forward genetic screen for cancer genes in mice (Copeland and Jenkins, 2010; DeNicola *et al*, 2015). We used this screening method to identify genes involved in the transformation of neural stem cells into glioma-initiating cells and identified DEAH (Asp-Glu-Ala-His) box helicase 15 (*Dhx15*) as a candidate tumour suppressor gene in glioma (Koso *et al*, 2012).

DHX15 is a member of the DEAH-box (DHX) RNA helicase family. A large number of RNA helicases have recently been identified. The human genome encodes 95 non-redundant helicase proteins, of which 64 are RNA helicases and 31 are DNA helicases (Umate *et al*, 2011). RNA helicase family proteins are involved in RNA metabolism, including pre-mRNA processing, transcription, translation, RNA folding, nuclear transport, RNA degradation, and RNA ribosomal complex formation (Patel and Donmez, 2006). RNA helicases are classified into two families based on their structural similarities: the DEAD-box (DDX) family proteins and the DHX family proteins (Umate *et al*, 2011). The DHX family consists of 16 members, which have been identified based on their homology within the helicase domain amino acid sequences (Umate *et al*, 2011; Suthar *et al*, 2016). Alignments of DHX protein sequences obtained from various organisms have revealed eight conserved motifs: I, Ia, Ib, II, III, IV, V, and VI (Tanner *et al*, 2003; Tuteja and Tuteja, 2004a, 2004b). Motifs I, II, and VI are necessary for nucleotide triphosphate (NTP) binding and hydrolysis

*Correspondence: Dr S Watanabe; E-mail: sumiko@ims.u-tokyo.ac.jp

Received 22 January 2017; revised 22 June 2017; accepted 24 July 2017; published online 22 August 2017

(Tanner *et al*, 2003; Tuteja and Tuteja, 2004b, 2006), whereas motifs Ia, Ib, IV, and V are involved in RNA binding (Svitkin *et al*, 2001). Motif III regulates the coupling of NTP hydrolysis with double-stranded RNA (dsRNA) unwinding (Tuteja and Tuteja, 2004b). RNA helicase family proteins control many biological processes, including cellular differentiation and apoptosis (Jiang and Wu, 1999). The involvement of DHX15 in immune responses has been reported (Mosallanejad *et al*, 2014; Wang *et al*, 2015). DHX15 regulates intestinal antiviral innate immunity through activation of the Nlrp6-interferon pathway (Wang *et al*, 2015). Conversely, DHX15 directly associates with MAVS (mitochondrial antiviral signal) protein and activates nuclear factor kappa B (NF-κB) and mitogen-activated protein kinase (MAPK) pathways during antiviral responses (Mosallanejad *et al*, 2014). RNA-binding motif protein 5, a tumour suppressor gene, directly interacts with DHX15 to stimulate its helicase activity (Niu *et al*, 2012). Recent studies have shown that deregulated expression of RNA helicase family proteins is commonly associated with cancer progression (Abdelhaleem *et al*, 2003; Fuller-Pace, 2006; Steimer and Klostermeier, 2012). Among the 60 helicases analysed, 11 are overexpressed in at least 10 different cancer types, while 4 are underexpressed (Robert and Pelletier, 2013). One of the best characterised RNA helicases is DDX3 (Bol *et al*, 2015). DDX3 facilitates the translation of mRNAs containing a long or structured 5′-untranslated region (UTR) (Lai *et al*, 2008; Soto-Rifo *et al*, 2012). DDX3 stimulates *Rac1* mRNA translation through its 5′-UTR, which in turn activates the WNT/β-catenin signalling pathway by preventing β-catenin from undergoing proteasome-dependent degradation (Chen *et al*, 2015). DDX3 also acts as a tumour suppressor by upregulating $p21^{WAF1/CIP1}$ expression through its transactivation function on the $p21^{WAF1/CIP1}$ promoter through an adenosine triphosphate (ATP) ase-dependent but helicase-independent mechanism (Chao *et al*, 2006). Deregulated expression of RNA helicase family proteins is frequently observed in many tumour types (Robert and Pelletier, 2013; Abdelhaleem, 2004a); however, the molecular mechanisms through which the dysregulation of RNA helicases contributes to tumourigenesis remain elusive for most RNA helicase proteins. In the present study, we investigated the role of DHX15 in glioma initiation. Our data strongly suggest that DHX15 functions as a tumour suppressor gene in glioma.

MATERIALS AND METHODS

Construction of retroviral expression vectors. Full-length *DHX15* was polymerase chain reaction (PCR)-amplified as described previously (Koso *et al*, 2016) using the following primers (F: 5′-TCC AGA GTT AAG TGG CTG TC-3′, R: 5′-TCC AGT ATG AGC TAC AGT GTC-3′). *DHX15* cDNA was inserted into the retroviral expression vector, pMXs-IRES-Puro (pMXs-IP) (Cell Biolabs, San Diego, CA, USA). To generate HA (Hemagglutinin)-tagged DHX15, N-terminal region of DHX15 was amplified with the following primers, and TA-cloned to the pGEM-T easy vector. F: 5′-CTC GAG ATG GGA TCC TAC CCT TAC GAC GTT CCT GAT TAC GCT AGC CTC GAA TTC TCC AAG CGG CAC CGG TTG-3′. R: 5′-TGA CGT GTG ACC TGC ATG TCC-3′. Plasmids with correct sequences were digested with restriction enzymes (*Xho*l and *Sph*l), and the resultant fragment was used to replace the N-terminal region of DHX15 to generate pMXs-HA-DHX15-IP. For short hairpin RNA (shRNA)-mediated *Dhx15* knockdown experiments, shRNA vectors were constructed as described previously (Koso *et al*, 2016). 22 nucleotides guide sequence for *Dhx15* is 5′-TTT CTT TAT AAG TTA TTT AAT T-3′ (sh1), 5′-TTT CTT TAG ATG ACT TAT TTA T-3′ (sh2), for Luciferase (non-targeting control) is 5′-ACC GCT TGA AGT CTT TAA TTA A-3′. The K166A and D260A mutants of human DHX15 were gifts from Dr Ichijo (Mosallanejad *et al*, 2014) (The University of Tokyo, Japan). Plasmids of pMXs-HA-DHX15-IP were digested with restriction enzymes (*Sph*l and *Sna*Bl), and we generated pMXs-HA-K166A-IP and pMXs-HA-D260A-IP. Deletion mutants of *DHX15* were generated using KOD -Plus- Mutagenesis Kit (Toyobo, Osaka, Japan). Inverse PCR of Plasmid DNA (pMXs-HA-DHX15-IP) was performed using the following primers (ΔIa F: 5′-GCT GCA ATG AGT GTG GCT CA-3′, R: 5′-ACA GGC AAC TCC TCT CTT GG-3′; ΔIb F: 5′-GAA GCT ATG AAT GAT CCC CT-3′, R: 5′-CAT ATA CTT AAG AAT GGT TTT TGC AC-3′; Δ Ia Ib F: 5′-CCT CCT GGA GCG TTA TGG TG-3′, R: 5′-AGG CAA CTC CTC TCT TGG GTC-3′; Δ3456 F: 5′-GCT TCA GAC TTT ACA CAG AG-3′, R: 5′-ACA ACT TCC TTC AGA ACA CC-3′). Plasmids with correct sequences were used for experiments.

Real-time PCR analysis. To analyse expression of *Dhx15* in neural stem cells and glioma, we used cDNA samples previously described (Koso *et al*, 2016). qPCR was performed using the following TaqMan assays (Invitrogen, Carlsbad, CA, USA). DHX15: Hs00154713_m1, GAPDH: Hs99999905_m1. To examine knockdown efficiency of *Dhx15* in primary astrocytes, total RNA was collected from primary immortalised astrocytes transduced with non-targeting shRNA and shRNA against *Dhx15* as described previously (Koso *et al*, 2016). First strand cDNA synthesis was performed using ReverTra Ace qPCR RT Master Mix with gDNA Remover (Toyobo) according to the manufacturer's protocol. qPCR was performed with the following primers using Light Cycler 96 (Roche, Basel, Switzerland). Primer for mouse *Dhx15*: sense, 5′-CAG AAT GGA GCA ATT GGA AGA-3′; antisense, 5′-TGT CAA AGA GGT CTC TGC AAT ATT AGT-3′; mouse and human *Gapdh*: sense, 5′-TGA CCA CAG TCC ATG CCA TC-3′; antisense, 5′-CAT ACC AGG AAA TGA GCT TGA-3′. Primers for human genes are: *RNPS1*: sense, 5′-GGA GAC TCA CCC GGA ATG TG-3′; antisense, 5′-TTC CAC GGG CAT GTC AAT CA-3′; *PRPF4*: sense, 5′-AGG ACC TCC CAG ATG CAA GA-3′; antisense, 5′-GCA AAG CCC ACT CCA ACA AG-3′; *SNRPB*: sense, 5′-GCT GGA CCG GAA GTA GGT TT-3′; antisense, 5′-CTC TCT CCC ACA GCC GAT TT-3′; *SF3B3*: sense, 5′-GCA CCT ACC ATG AAC CAC CA-3′; antisense, 5′-CCT CAC AGC GAC AGA GAC TG-3′; *PHF5A*: sense, 5′-GGT GTG TGG TGG GAA GCT AT; antisense, 5′-CCC CAC TGT AGC TGG ACA AG-3′; *FUS*: sense, 5′-AGG AGG TCG AAG CTC CTT GT-3′; antisense, 5′-CCC AAA CTG GAC CTA CCC AC-3′; *IRF1*: sense, 5′-AAG GGG TGT GGC CTT TTT AGA-3′; antisense, 5′-TGT CCC TGT TCA CCC CAA AG-3′; *IRF3*: sense, 5′-CCT GCA CAT TTC CAA CAG CC-3′; antisense, 5′-AAT CCA TGC CCT CCA CCA AG-3′; *IRF7*: sense, 5′-GCT CCC CAC GCT ATA CCA TC-3′; antisense, 5′-CAG GGA AGA CAC ACC CTC AC-3′; *NFKB1*: sense, 5′-GTG AAG ACC ACC TCT CAG GC-3′; antisense, 5′-CTG TCG CAG ACA CTG TCA CT-3′; *NFKB2*: sense, 5′-ACG CCT CTT GAC CTC ACT TG-3′; antisense, 5′-GTG GCT CCA TGG TGT TCT GA-3′; *RELA*: sense, 5′-GGA CAT GGA CTT CTC AGC CC-3′; antisense, 5′-AAA GTT GGG GGC AGT TGG AA-3′; *REL*: sense, 5′-TCC TTA GCC CAG CCA TCT CT-3′; antisense, 5′-GGC AGT CTC CGC TCA TCT TT-3′. Primers for mouse genes are; *Rnps1*: sense, 5′-AGC TCC AAC TCC TCC CGA TA-3′; antisense, 5′-TCT ACA GAC CCT CAC TTG GCT-3′; *Prpf4*: sense, 5′-TCT CAC GAC GGA GCC ATT TC-3′; antisense, 5′-CAG GCT TCC TCA AGA GTG GG-3′; *Snrpb*: sense, 5′-GCA GGC AGC ATT TCC GTT AG-3′; antisense, 5′-CAG CAT CTT GCT GCT CTT GC-3′; *Sf3b3*: sense, 5′-TCC ATG GAA CCC AAC AAG CA-3′; antisense, 5′-CTG GCA AGG CCC CAG ATA AA-3′; *Phf5a*: sense, 5′-AAA GTT GGC TAC CTT CCC CG-3′; antisense, 5′-TCT GCC CGT CCA TCA TTA GC-3′; *Fus*: sense, 5′-TGC AAC CAG TGT AAG GCA CC-3′; antisense, 5′-GCC ACG TCG ATC ATC TCC-3′ AT; *Irf1*: sense,

5′-AAA GTC CAA GTC CAG CCG AG-3′; antisense, 5′-AGC CCT GAG TGG TGT AAC TG-3′; *Irf3*: sense, 5′-CTA CAC CCC GGG GAA GGA TA-3′; antisense, 5′-CTT CTT TCC GGT TCA GGG CT-3′; *Irf7*: sense, 5′-TGG AAG ACC AAC TTC CGC TG-3′; antisense, 5′-TCC CTA TTT TCC GTG GCT GG-3′; *Nfkb1*: sense, 5′-GAG GTC TCT GGG GGT ACC AT-3′; antisense, 5′-AAG GCT GCC TGG ATC ACT TC-3′; *Nfkb2*: sense, 5′-GAT GAA GAT CGA GAG GCC TGT AA-3′; antisense, 5′-GCT TCC TCT GCA CTT CCT CCT T-3′; *Rela*: sense, 5′-ATC ATC GAA CAG CCG AAG CA-3′; antisense, 5′-GTT CCT GGT CCT GTG TAG CC-3′; *Rel*: sense, 5′-TAC TCG GCC TCT GAG TGT GA-3′; antisense, 5′-GGC CTA GCC TGG CAT TAC AT-3′. We used the primers previously reported for human *CDKN1A, CDKN1B, CDKN1C, CDKN2A, CDKN2B, CDKN2D, ATCB* (Koso *et al.*, 2016). The expression profiling of glioma stem cells was performed with the institutional approval (Institute of Medical Science, University of Tokyo).

Glioma cell lines. Three human glioma cell lines were obtained from the American Type Culture Collection (ATCC): U-87MG (ATCC HTB-14), U-118MG (ATCC HTB-15), and U-138MG (ATCC HTB-16). All cell lines tested negative for *mycoplasma* contamination. The lines were authenticated by standard morphological examination using microscopy. The glioma cell lines were cultured in DMEM containing 10% FBS and penicillin-streptomycin. Cell line authentication was performed for U-87MG, U-118MG, and U-138MG cell lines by using the short tandem repeat (STR) profiling service (Promega, Madision, WI, USA). It should be noted that U-118MG and U-138MG cell lines generated the same STR profile because they are derived from the same patient (Bady *et al*, 2012).

Retroviral infection. Retroviral infection was performed as described previously (Koso *et al*, 2016). Briefly, 2×10^5 glioma cells were incubated with retroviral solutions. After 2 days, infected cells were selected with puromycin ($2\,\mu g\,ml^{-1}$) for 5 days and used for the subsequent analysis. For experiments using primary astrocytes, primary astrocytes that overexpresses p53DN and shRNA against *Nf1* were used (Koso *et al*, 2016). For intracranial injections, U-87MG cells that were retrovirally transduced with EGFP (pMXs-IRES-EGFP vector) were used.

Cell proliferation assay. 5×10^4 of *Dhx15*-transduced or the control empty vector-transduced cells were plated on 6 well plate triplicate. The morphology of the cells was analysed on day 1, 3, and 5. The total number of cells was counted on day 5. Total cell counts were obtained by using a hemocytometer.

Foci formation assay. Five hundred cells of the *Dhx15*-tran or the control empty vector-transduced cells were plated in 10 cm dish. The cells were stained by 2% methylene blue in 60% methanol at 2–3 weeks later. The total number of colonies was counted. Viable cell counting was performed by using the Trypan Blue exclusion method.

Western blot analysis. Cell lysates were collected from *Dhx15*-transduced or the control empty vector-transduced cell lines (2×10^6 cells) and used for Western blotting. Primary antibodies against HA (Covance, Princeton, NJ, USA), actin (Sigma, St Louis, MO, USA), DHX15 (Atlas Antibodies AB, Voltavagen, Sweden) and HRP-linked secondary antibodies (GE Healthcare, Little Chalfont, England) were used. Band intensities were measured by using Image J software.

Immunocytochemistry and immunohistochemistry. Cells were fixed with 4% paraformaldehyde (PFA) and permeated with 70% ethanol. Following primary antibodies were used. Mouse monoclonal antibody against HA (MBL), Mouse monoclonal antibody against Ki67 (BD), Rabbit polyclonal antibody against active Caspase 3 (AC3) (Promega) was used. EdU staining was performed using Click-iT Assay Kits (Invitrogen) according to the manufacturer's protocol. Nucleus was counter-stained with DAPI. Stained cells were observed with an inverted fluorescence light microscope (Zeiss, Oberkochen, Germany), and images were acquired with AxioImager software. Immunohistochemistry was performed as described previously (Koso *et al.*, 2016). Briefly, tissues were fixed with 4% PFA. Sections of 10 μm were prepared by using Cryostat (Leica, Wetzlar, Germany). Ki67 and AC3 staining was performed using the above-mentioned antibodies. GFP staining was performed using a rat monoclonal antibody (Nacalai Tesque, Kyoto, Japan). EdU staining was performed according to the manufacturer's protocol.

Animal experiments. A total of 1×10^7 of control U-87MG cell lines transduced with the empty vector control, or DHX15 were injected subcutaneously into the flank of six female nude mice at 7 weeks of age. The size of each tumour was measured every week and the tumour volume was estimated by multiplying the length, width, and height. For intracranial transplantation, 2×10^5 cells were injected into the striatum of female nude mice at 7 weeks of age. After 6 days, histologic analyses were performed. EdU ($50\,mg\,kg^{-1}$) was intraperitoneally administered for 2 consecutive days before sacrifice. All animal experiments were performed following the animal welfare guideline (Workman *et al*, 2010). All procedures were performed with the institutional approval (IMSUT).

Analysis of the cancer genome atlas datasets. Analysis was performed as reported previously (Koso *et al*, 2016). Briefly, a total of 565 glioblastoma primary tumour cases from The Cancer Genome Atlas (TCGA) were analysed, all of which had genome-wide copy-number profiling; of these, 283 cases had associated exome sequencing data (Broad Institute analysis run from December 17, 2014; doi:10.7908/C10V8BNC). The original TCGA data contains copy number variations given as values -2, -1, 0, $+1$, $+2$. The terms 'heterozygous deletion' and 'homozygous deletion' were assigned to -2 (deep loss) and -1 (shallow loss), respectively.

RESULTS

***Dhx15* is a candidate tumour suppressor gene in glioma.** Using the transposon-mediated mutagenesis approach, we identified *Dhx15* as a tumour suppressor candidate gene in mouse glioma (Koso *et al*, 2012). Insertions within the *Dhx15* locus were distributed throughout the gene, and there was little orientation bias (Figure 1A), suggesting its tumour suppressor function. To compare the expression levels of *DHX15* between normal neural stem cells and glioma, we used three neural stem cells that have differentiated from human induced pluripotent stem or embryonic stem cells (Koso *et al*, 2016), three glioma stem cells (Ikushima *et al*, 2009), and six glioma cell lines (U-87MG, U-118MG, U-138MG, U-251MG, T98G, and A172). Real-time PCR analysis revealed that *DHX15* expression was downregulated in glioma compared with that in normal neural stem cells (Figure 1B), consistent with its putative tumour suppressor function. Analysis of copy number alterations at the *DHX15* gene locus using TCGA database showed that homozygous and heterozygous deletions of *DHX15* were detected in 0.2% and 10.4% of 565 GBM patient samples, respectively. These findings strongly suggest the tumour suppressor function of DHX15 in human glioma.

***Dhx15* knockdown promotes the proliferation of immortalised astrocytes.** For a functional analysis, we first examined the effects of *Dhx15* knockdown on the proliferation of primary astrocytes. Primary astrocytes immortalised with *p53* dominant-negative (DN) and shRNA against the *Nf1* tumour suppressor gene were

examined (Koso *et al*, 2016). We used immortalised astrocytes, rather than glioblastoma cell lines, because weaker tumourigenicity of immortalised astrocytes then glioblastoma cell lines allowed us to examine the growth-promoting effect of additional genetic alterations more easily than glioblastoma cell lines. The immortalised astrocytes were infected with retroviruses encoding shRNA against luciferase (Luc), or first or second shRNA against *Dhx15*. Real-time PCR confirmed the shRNA-mediated knockdown of *Dhx15* in immortalised astrocytes (Figure 1C). Western blot analysis further confirmed ~50% reduction in the expression level of DHX15 protein (Figure 1D), modelling DHX15 haploinsufficiency. Cell growth was then determined by counting the cell number using a hemocytometer in the culture (Supplementary Figure 1a). Knockdown of *Dhx15* resulted in approximately 40% to 50% increases in the cell number of immortalised astrocytes (Figure 1E), supporting that DHX15 acts as a tumour suppressor in glioma. Although we performed xenograft experiments, these cells were not tumourigenic, suggesting that additional changes are required to fully transform these cells.

DHX15 overexpression suppresses the proliferation of three glioma cell lines. We then overexpressed DHX15 and, for this purpose, generated a human influenza HA-tagged DHX15 construct (Figure 2A). HA-DHX15 was retrovirally transduced into glioma cell lines and puromycin-resistant cells were selected. Western blot analysis confirmed the expression of HA-DHX15 in transfected glioma cells (Figure 2B). Immunocytochemistry showed that DHX15 was mainly located within the nucleus of transfected U-118M, U-138MG, and U-87MG cells (Figure 2C). We next examined its effects on cell growth using U-118MG, U-138MG, and U-87MG glioma cells. The same number of cells that were transduced with either the empty vector control or HA-DHX15 were plated (Supplementary Figure 2a), and the total cell number was counted on day 5 after plating. In all cases, overexpression of HA-DHX15 significantly suppressed the cell number increase compared with that in control glioma cells (Figure 2D). For further confirmation of the growth-inhibitory effect of DHX15, we performed a foci formation assay. Control- or HA-DHX15-transduced U-118MG, U-138MG, and U-87MG glioma cell lines were plated at a low density. After 2–3 weeks in culture, the total number of foci was counted. DHX15 overexpression suppressed foci formation in all three glioma cell lines (Figure 2E; Supplementary Figure 2b). The number of Ki67-positive proliferating cells was significantly reduced after DHX15 transfection (Figure 3A–C), whereas the number of AC3-positive apoptotic cells was comparable between control and DHX15-tranfected cells (Figure 3D–F). Taken together, these findings indicate that DHX15 suppressed growth of glioma cell lines by reducing proliferation.

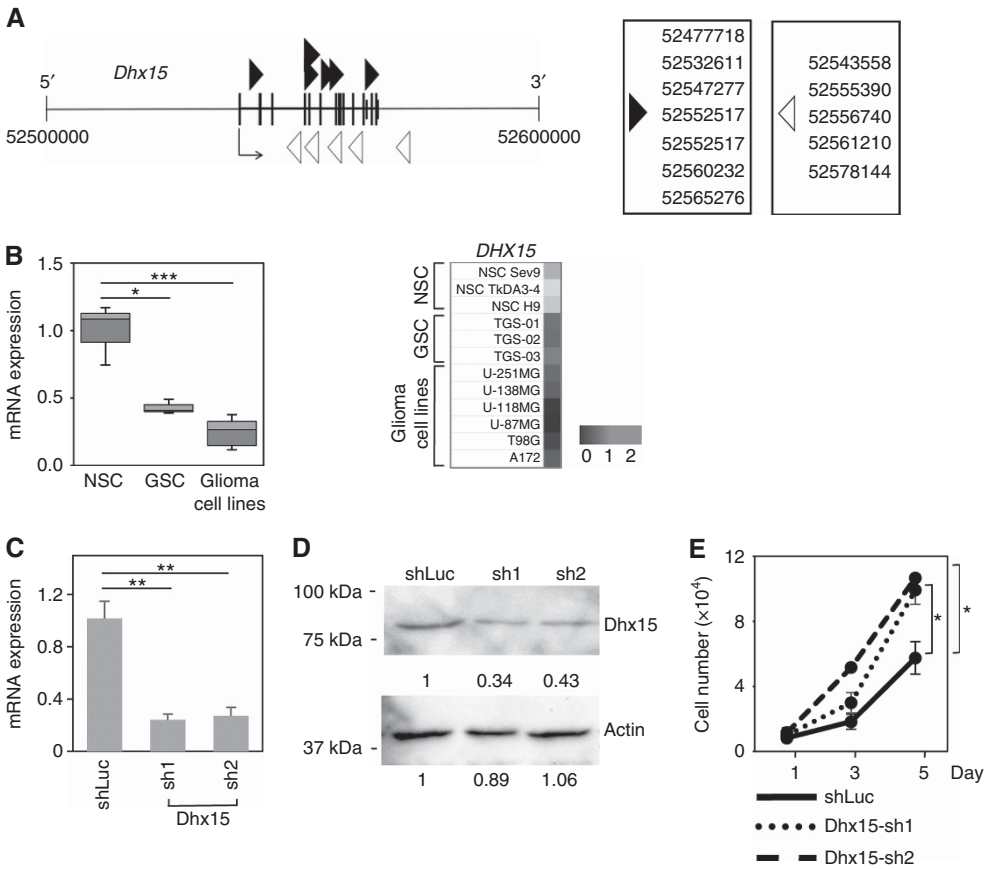

Figure 1. Dhx15 is a tumour suppressor candidate gene in glioma. (**A**) The pattern of transposon insertions in the *Dhx15* gene locus. Insertion size is 2050 bp. Transposon insertions are located in the sense (black arrowheads) or antisense orientation (white arrowheads) relative to transcription. The positions of transposon insertions are shown. (**B**) Expression levels of *DHX15* were compared between three neural stem cells and glioma samples (i.e., three glioma stem cells and six glioma cell lines). Expression levels are visualised in a heatmap. Data represent mean ± s.e.m. Student's *t* test $*P<0.05$, $***P<0.001$ (two-tailed). (**C**, **D**) The *p53* and *Nf1*-deficient astrocytes were infected with retrovirus that expresses shRNA against Luciferase (shLuc) or *Dhx15* (sh1 and sh2). *Dhx15* mRNA expression levels were normalised by *Gapdh* (**C**). Data represent mean ± s.e.m. Student's *t* test $**P<0.01$ (two-tailed). Dhx15 protein expression levels are shown in (**D**). (**E**) Proliferation of primary astrocytes after a *Dhx15* knockdown. The total cell number was counted on day 1, 3, and 5 after plating. Bars represent 200 μm. Data represent mean ± s.e.m. ($n=3$ per group). One-way ANOVA with the Bonferroni correction for multiple testing, $*P<0.05$. Data are representative of two independent experiments.

DHX15 overexpression suppresses the proliferation of glioma cells *in vivo*. We next analysed the effect of DHX15 overexpression on glioma cell growth *in vivo*. Ten million control- or DHX15-transfected U-87MG and U-118MG cells were subcutaneously transplanted into nude mice. U-87MG cells generated tumours, whereas U-118MG cells were not tumourigenic (Figure 4A, Supplementary Figure 3a). After 3 weeks, the mice that harbour tumours were sacrificed and the tumours isolated, and tumour volume was examined (Figure 4A). DHX15 transduction significantly reduced the size of subcutaneous tumours at 3 weeks after transplantation (Figure 4B), indicating that DHX15 suppresses glioma cell growth *in vivo*. Although we compared proliferation and apoptosis between control and DHX15-transfected tumours, Ki67- and AC3-positive cells were comparable at this stage, suggesting that the growth-inhibitory effect of DHX15 is transient (Supplementary Figure 3b, c). Intracranial injection of the control U-87MG cells induced clusters of glioma cells in the brain on day 6 after transplantation, and these cells incorporated EdU, indicating that control U-87MG cells proliferated in the brain (Supplementary Figure 4). In sharp contrast, DHX15-transfected cells gave small clusters in the brain compared to the control, and EdU+ proliferating cells were hardly observed (Supplementary Figure 4). These data indicate that DHX15 suppressed tumour cell growth in the brain.

ATPase activity is not required for the growth-inhibitory effect of DHX15. DXH15 is reported to exhibit ATPase activity. We therefore investigated whether the ATPase activity of DHX15 is required for its growth-inhibitory effect. The K166A and D260A mutants of DHX15 lacking ATPase activity were examined (Mosallanejad *et al*, 2014) (Figure 5A). DHX15 (K166A) and DHX15 (D260A) were retrovirally transduced into glioma cell lines. Western blot analysis confirmed the expression of these mutant proteins (Figure 5B). We next performed proliferation assays. Overexpression of the ATPase-deficient mutants suppressed the proliferation of U-118MG and U-138MG glioma cell lines in a manner similar to that of wild-type DHX15 (Figure 5C). These findings suggest that DHX15 suppresses the proliferation of glioma cells in an ATPase-independent manner.

Motifs Ia–Ib and III–IV of DHX15 play important roles in the growth-inhibitory function of DHX15. Because DXH15 contains eight conserved motifs (I, Ia, Ib, II, III, IV, V, and VI), as observed with other DHX helicase family protein members, we aimed to

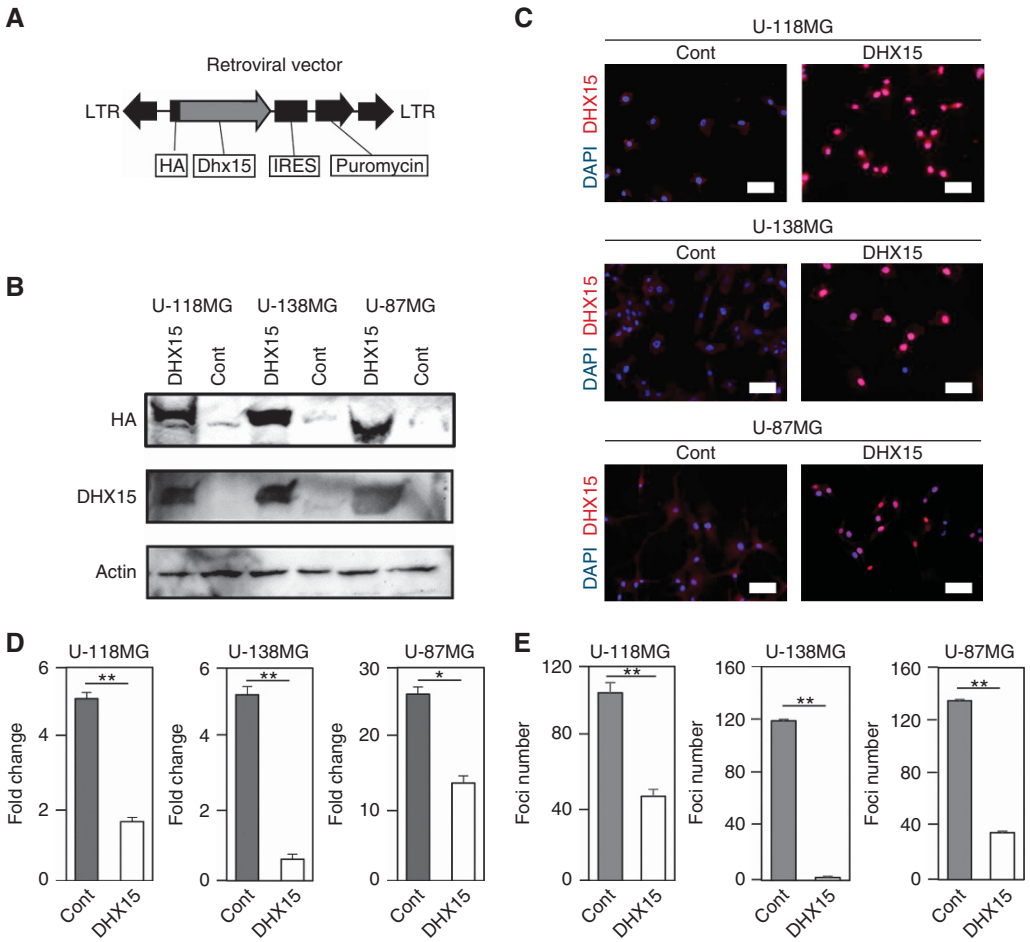

Figure 2. DHX15 overexpression reduced proliferation of three glioma cell lines. (**A**) Schematic drawing of HA-tagged DHX15. (**B**) Western blot analysis of HA-DHX15 expression in U-118MG, U-138MG, and U-87MG cells. The empty vector was used as control. (**C**) U-118MG, U-138MG, and U-87MG glioma cell lines that were transduced with HA-DHX15 were stained with an anti-HA antibody. DAPI was used to counterstain the nucleus. Bars represent 200 μm. (**D**) U-118MG, U-138MG, and U-87MG glioma cell lines were retrovirally transduced with HA-DHX15 or the empty vector control (cont) and used for proliferation assays. The same number of infected cells was plated (day 0), and the morphology of the cells was observed on day 5. The fold change was calculated on day 5 (The total number of cells on day 5 was divided by the number of cells plated on day 0). Data represent mean ± s.e.m. ($n=3$ per group). Student's t test $^*P<0.05$, $^{**}P<0.01$ (two-tailed). (**E**) The above-mentioned glioma cells were used for the focus formation assay. The total number of foci was counted 2 ~ 3 weeks after plating. Data represent mean ± s.e.m. ($n=3$ per group). Student t test (2-tailed), $^{**}P<0.01$. Data are representative of two independent experiments.

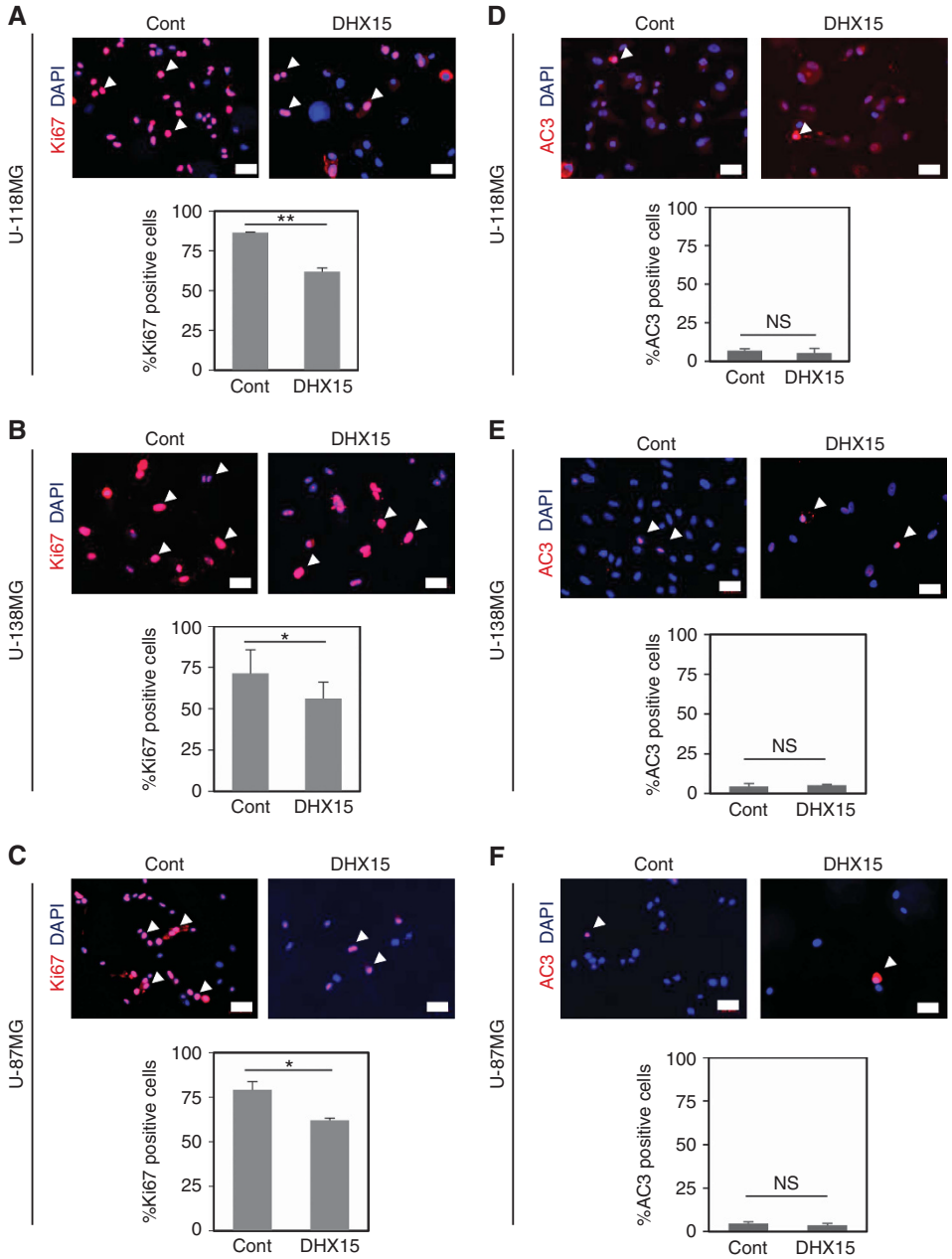

Figure 3. DHX15 overexpression suppressed glioma cell proliferation *in vitro*. (**A**–**C**) Analysis of Ki67+ proliferating cells in U-118MG (**A**), U-138MG (**B**), and U-87MG (**C**) glioma cell lines that were transduced with HA-DHX15 or the vector control (cont). The analysis was performed on day 1 after plating. Arrowheads point to Ki67+ cells. (**D**–**F**) Analysis of AC3+ apoptotic cells in U-118MG (**D**), U-138MG (**E**), and U-87MG (**F**) glioma cell lines that were transduced with the vector control (cont) of HA-DHX15 (DHX15). The analysis was performed on day 1 after plating. Arrowheads point to AC3+ cells. DAPI was used to counterstain the nucleus. Bars represent 50 μm. ($n=3$ per group). Student *t* test (one-tailed), $^{*}P<0.05$, $^{**}P<0.01$.

determine which motif(s) is essential for the growth-suppressive function of DHX15. We constructed internal deletion mutants lacking distinct motifs (Figure 5A), and western blot analysis confirmed the expression of the mutant DHX15 proteins at their expected molecular weights (Figure 5B). The mutants were then retrovirally transduced into U-138MG glioma cell lines, and cell growth was determined by counting the cell number. ΔIaIb lacks both Ia and Ib motifs; ΔIaIb failed to suppress the growth of U-138MG glioma cell lines (Figure 5D). Δ3456 lacks motifs III, IV, V, and VI; overexpression of this mutant enhanced the growth of U-138MG glioma cell lines (Figure 5D; Supplementary Figure 5a). We then investigated whether Ia or Ib is required for DHX15 activity by introducing mutants lacking either motif (HA-ΔIa or HA-ΔIb, respectively). Neither HA-ΔIa nor HA-ΔIb affected the growth-suppressive function of DHX15 (Figure 5E; Supplementary Figure 5b), suggesting that motifs Ia and Ib function redundantly. Motifs Ia and Ib exert RNA-binding ability (Svitkin *et al*, 2001), suggesting that interactions with RNA are involved in the growth-inhibitory function of DHX15.

DHX15 dysregulates NF-κB signal pathway, splicing, and ribosomal biogenesis in glioma. We analysed molecular mechanisms responsible for the growth-inhibitory effects of DHX15. We first examined expression of cyclin-dependent kinase (CDK) inhibitors, because a previous study reported that DDX3 acts as a tumour suppressor by upregulating *CDKN1A* expression through

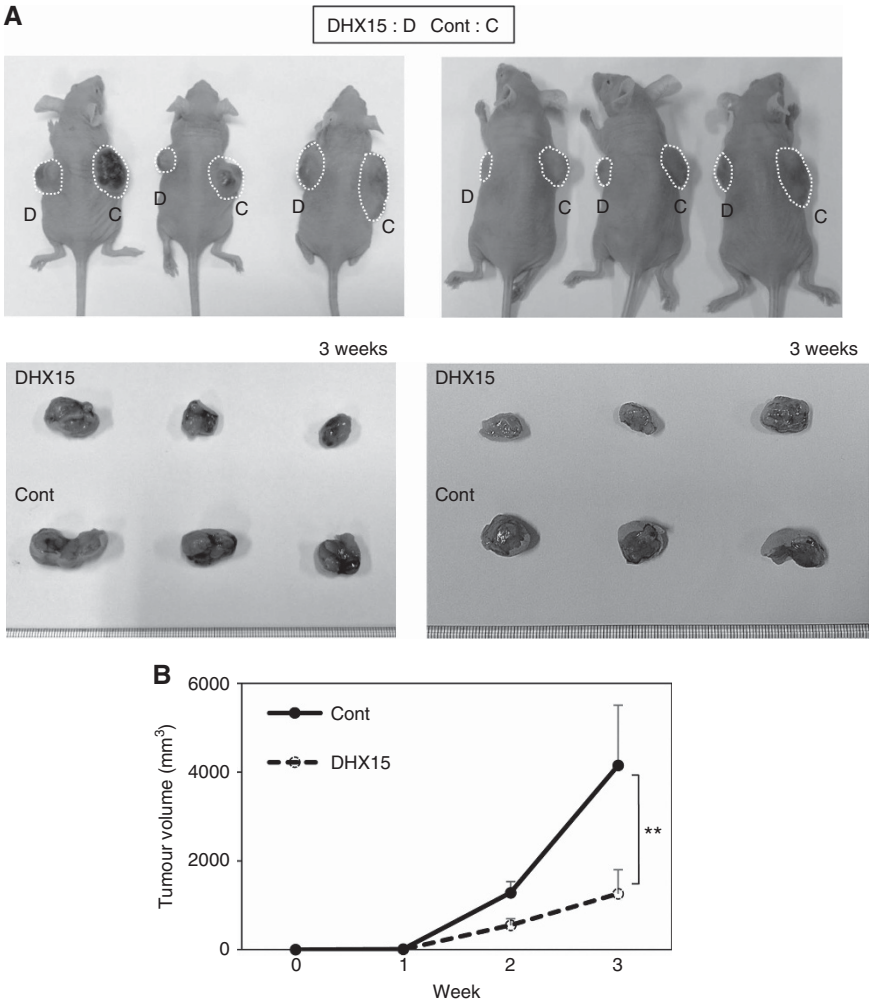

Figure 4. DHX15 overexpression suppressed glioma cell growth *in vivo*. (**A**, **B**) Subcutaneous tumours derived U-87MG cell line transfected with the empty vector or DHX15. Tumour size was monitored until 3 weeks after injection. Millimeter ruler is shown at the bottom. Data represent mean ± s.e.m. ($n = 6$ per group). Student *t* test (one-tailed), $^{**}P < 0.01$.

its transactivation function on the *CDKN1A* promoter (Chao *et al*, 2006). In addition, we reported that LARP4B suppressed glioma cell growth through upregulation of *CDKN1A* (Koso *et al*, 2016). Thus, we first asked involvement of CDK inhibitors by examining their expression levels in the glioma cells transfected with DHX15. None of the CDK inhibitors were upregulated by DHX15 transfection (Figure 6A), indicating that DHX15-mediated growth-inhibition is not due to the upregulation of CDK inhibitors. A previous study showed that DHX15 overexpression resulted in the activation of the NF-κB reporter in HEK293 cells, suggesting that DHX15 promoted the transcriptional activity of NF-κB (Mosallanejad *et al.*, 2014). To investigate DHX15 similarly activates NF-κB signalling in glioma cells, we examined expression levels of the genes downstream of NF-κB, including *IRF1*, *IRF3*, *IRF7*, *NFKB1*, *NFKB2*, *REL*, *RELA* (Marta and Marek, 2015). Upregulation of the genes was not observed, and they were rather suppressed by the overexpression of DHX15 in glioma cells after DHX15 transfection (Figure 6B). There results suggested that DHX15 suppressed NF-κB signalling in glioma cells, which is supposed to be one of mechanisms of DHX15 tumour suppressor function. We also performed RT-qPCR analysis of the genes downstream of NF-κB using the astrocytes transfected with Dhx15 shRNA. Dhx15 knockdown did not upregulate NF-κB downstream genes (Supplementary Figure 6a), indicating that DHX15 expression and NF-κB suppression were not correlated. DHX15 was reported to regulate disassembly of the spliosome (Bourgeois *et al*, 2016). A recent study revealed that DHX15-knockdown affected expression levels of the genes involved in splicing (including *RNPS1*, *SF3B3*, *PRPF4*) and ribosomal biogenesis (including *SNRPB*, *FUS*, *PHF5A*) in HEK293T cells (Faber *et al*, 2016). Thus, we examined the expression levels of these genes in the astrocytes transfected with Dhx15 shRNA. Both the genes involved in splicing and ribosomal biogenesis were slightly upregulated after Dhx15 knockdown but the differences were not statistically significant (Supplementary Figure 6b). We next examined expression levels of these genes in glioma cells transfected with DHX15. Interestingly, expression levels of *SF3B3*, *PRPF4*, and *SNRPB* were significantly downregulated, and level of other genes were also lowered although they are not statistically significant after DHX15 transfection (Figure 6C). These results suggested that the DHX15 has global role(s) for regulating mRNA of certain subsets of genes probably through regulation of splicing or turnover.

DISCUSSION

Accumulating evidence suggests that DEAH-box (DHX) RNA helicases play important roles in cancer (Abdelhaleem, 2004b). In the present study, we focused on DHX15 and revealed its role as a tumour suppressor. Genetic examination of *DHX15* in human GBMs available in TCGA database showed that there was a

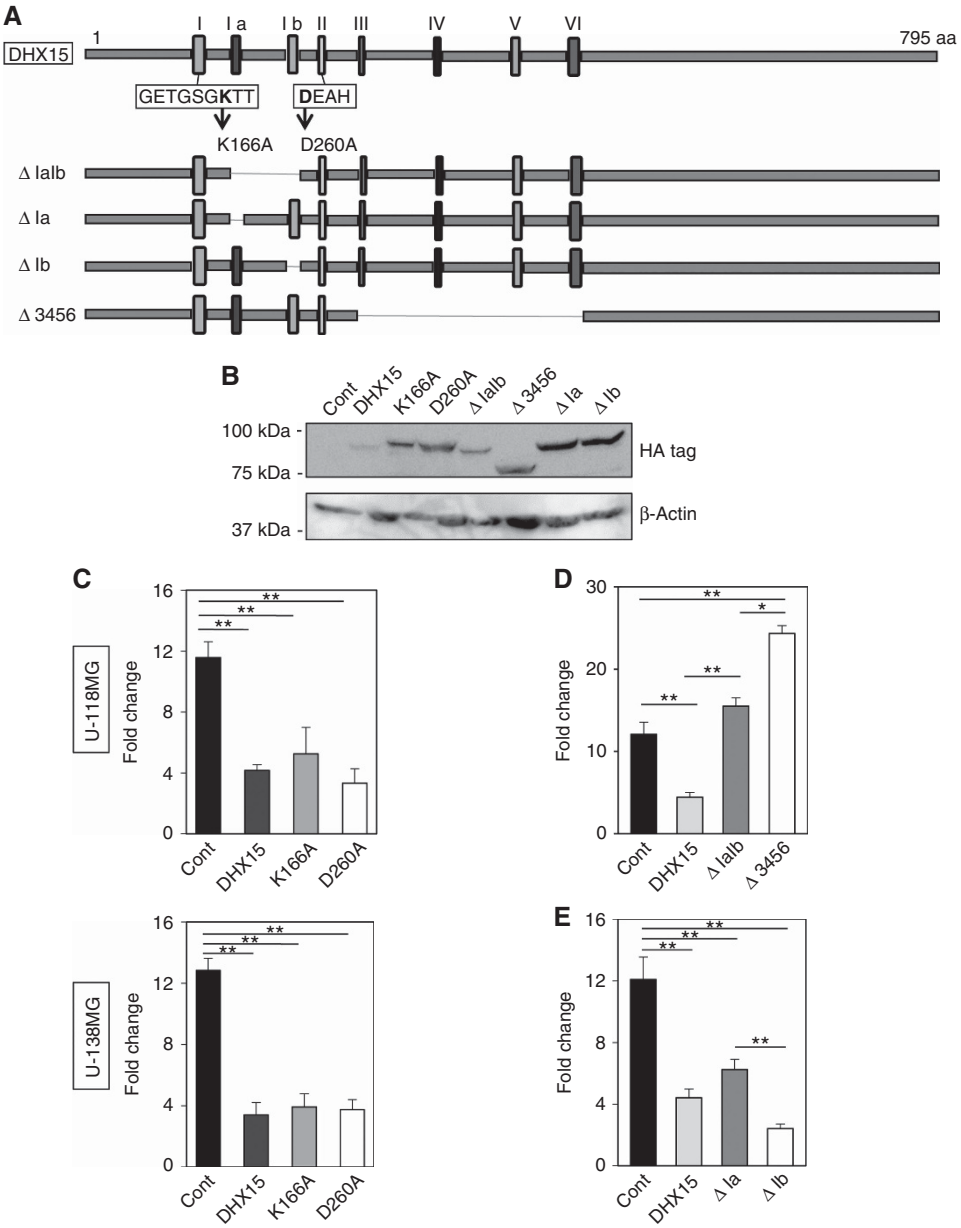

Figure 5. The motifs Ia and Ib play important roles in the growth-inhibitory function of DHX15. (**A**) A cartoon depicting the motif structure of DHX15 and mutants carrying deletions of individual motifs. Schematic representation of the primary structure of DHX15 protein. The amino acid residues that were mutated to alanine to generate ATPase-deficient mutants of DHX15 are shown (K166A and D260A) (Mosallanejad *et al*, 2014). (**B**) Western blot analysis of mutant DHX15 proteins in U-138MG glioma cells. The empty vector was used as control. (**C**) Glioma cells were retrovirally transduced with the vector control (cont), HA-DHX15, HA-K166A, or HA-D260A and used for proliferation assays. The same number of infected cells was plated (day 0), and the morphology of the cells was observed on day 1, 3, and 5. The fold change was calculated on day 5. Data represent mean ± s.e.m. ($n = 3$ per group). (**D**, **E**) U-138MG glioma cells were retrovirally transduced with the empty vector control, HA-DHX15, HA-ΔIaIb, HA-Δ3456, HA-ΔIa, HA-ΔIb and used for proliferation assays. The same number of infected cells was plated (day 0), and the morphology of the cells was observed on day 5. The fold change was calculated on day 5. Data represent mean ± s.e.m. ($n = 3$ per group). One-way ANOVA with the Bonferroni correction for multiple testing, $^{*}P < 0.05$, $^{**}P < 0.01$.

heterozygous deletion of *DHX15* in ~10% of 565 GBM patient samples.

A fundamental cellular function of RNA helicases is to unwind nucleic acid duplexes in RNA metabolism (Suthar *et al*, 2016). The energy of ATP hydrolysis is required for an active unwinding process (Umate *et al*, 2011). DHX15 has been assigned specific roles in disassembling the spliceosome after the second catalytic step by dissociating the U5 small nuclear ribonucleoprotein and the spliced mRNA (Koodathingal *et al*, 2010). The ATPase action of DHX15 is required and sufficient for spliceosome dissociation (Fourmann *et al*, 2013). However, we found that the ATPase activity of DHX15 is not required for its growth-inhibitory effect, suggesting that the disassembly of the spliceosome is not involved in the growth-inhibitory effects of DHX15 in glioma.

In contrast, the growth-suppressive function of DHX15 was greatly impaired by the deletion of motifs Ia and Ib (ΔIaIb) or III through VI (Δ3456). Motifs Ia, Ib, IV, and V have RNA-binding ability (Svitkin *et al*, 2001), suggesting that interactions between DHX15 and RNA may play an important role in the growth-inhibitory function of DHX15. The amino acid sequences of motifs

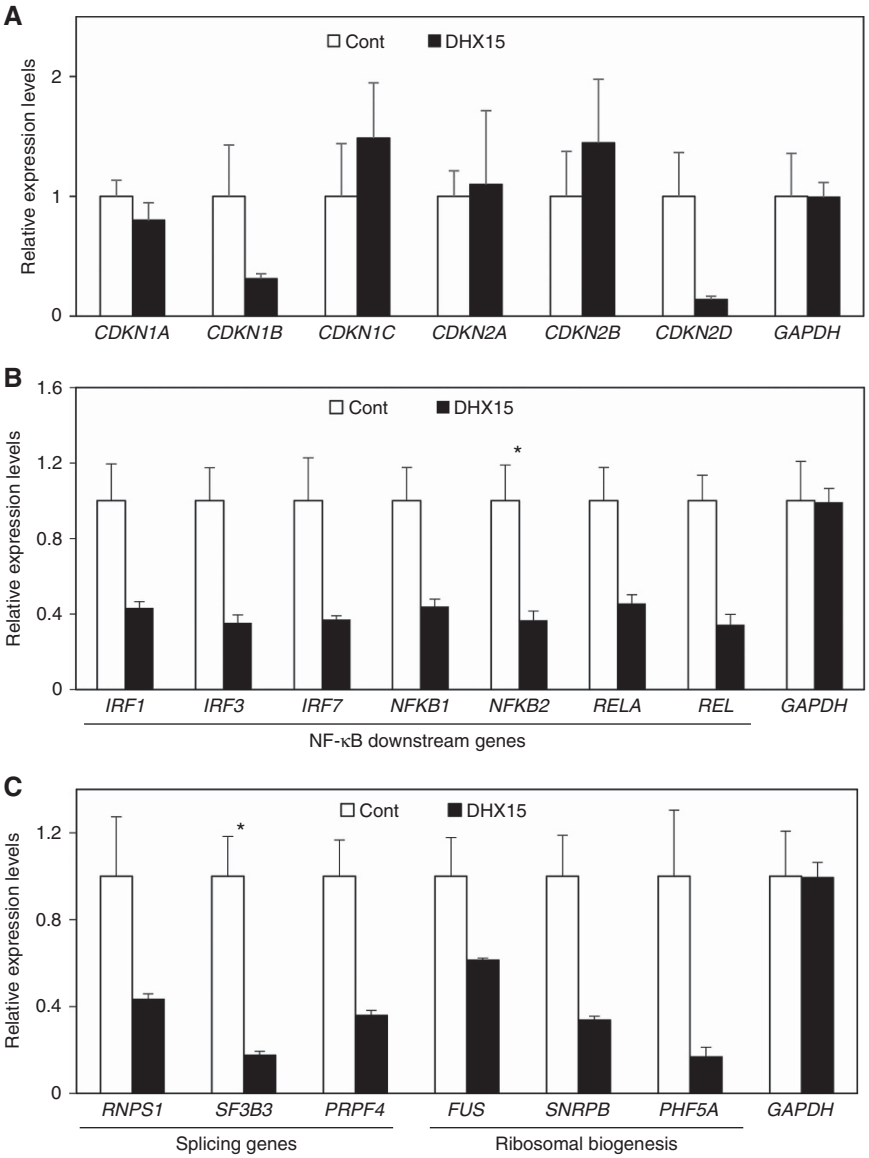

Figure 6. Analysis of gene expression changes induced by DHX15. (**A**–**C**) Expression levels of CDK inhibitors (**A**), NF-κB downstream target genes (**B**) and the genes involved in splicing and ribosomal biogenesis (**C**) were analysed using U-87MG glioma cell lines that were retrovirally transduced with HA-DHX15 or the empty vector control (cont). The qPCR analysis was performed on day 1 after plating. Expression levels were normalised by *Actb*. Data represent mean ± s.e.m. ($n = 3$ per group). Student *t* test (one-tailed), $^*P < 0.05$.

Ia and Ib share only 22% homology; therefore we speculate that these motifs may not be redundant and function complementarily or coordinately. It should be noted that we cannot exclude the possibility that deleting parts of the DHX15 rendered the protein inactive or dominant negative. By directly interacting with RNAs, DHX15 may affect alternative splicing or stability of its target RNAs. Interestingly, we observed downregulation of the genes involved in splicing after DHX15 transduction in glioma. A recent study reported a recurrent *DHX15* mutation (R222G) in RUNX1-RUNX1T1 acute myeloid leukaemia (Faber *et al*, 2016). Although whether the R222G mutation results in gain- or loss-of-function of DHX15 remains unknown, R222G mutant increased the number of alternative splicing events in HEK293T cells. Furthermore, it was shown that overexpression of wild-type DHX15 affected expression levels of the genes involved in splicing and ribosomal biogenesis in HEK293T cells (Faber *et al*, 2016). These results suggested that dysregulated splicing machinery may be a part of mechanisms of DHX15 tumour-suppressive effects. However, since depletion of DHX15 in astrocyte did not clearly upregulate expression levels of these genes, and deregulated expression of these genes may not be the primary cause of tumourigenesis by the loss of DHX15.

On the other hand, DHX15 participates in the antiviral response through its ATPase-independent function (Mosallanejad *et al*, 2014). In this response, DHX15 directly binds to dsRNA, forms a complex with MAVS, and mediates MAVS-dependent apoptosis through activation of the NF-κB pathways (Lu *et al*, 2014). Importantly, we showed that expression levels of the downstream target genes of the NF-κB pathway were not upregulated by DHX15 transfection, indicating that DHX15 did not activate NF-κB pathway in glioma cells. These data are consistent with the result that apoptosis was not induced by DHX15 in glioma cells, supporting the notion that MAVS and its downstream NF-κB pathway are not involved in the phenotype observed in the current work by DHX15. Interestingly, some of the NF-κB downstream target genes were downregulated by DHX15 transfection. NF-κB

activation has been implicated as an important driver of the malignant phenotype that confers a negative prognosis in patients with GBM (Korkolopoulou *et al*, 2008; Bhat *et al*, 2013). In fact, NF-κB pathway functions as a survival signal in U87-MG cells (Zhang *et al*, 2007). Therefore, suppression of NF-κB pathway in glioma cells may have contributed to the growth inhibition induced by DHX15. However, shRNA-mediated DHX15 depletion did not upregulate NF-κB targets in astrocyte. Therefore, it is not plausible that NF-κB activation is the primary mechanism, through which DHX15 loss promotes tumourigenesis.

Interestingly, a deletion mutant lacking motifs III–VI promoted the proliferation of glioma cells compared with wild-type DHX15. One possible explanation for this is that the Δ3456 mutant functions as a dominant-negative form of DHX15 and suppresses the growth-inhibitory effect of wild-type DHX15. As described above, motif III (SAT) is involved in the coupling of ATP hydrolysis and unwinding; motifs IV (FLTG) and V (TNIAET) are involved in RNA binding; and motif VI (QRAGRAGR) is required for nucleic acid-dependent NTP hydrolysis (Tuteja and Tuteja, 2004b, 2006). These motifs have never been reported as having tumour-suppressive functions. To understand the relative roles of these motifs in tumour suppression remains a task for the future analysis.

ACKNOWLEDGEMENTS

We are grateful to all the members of the Laboratory for their crucial comments. This work was supported by the Japan Society for the Promotion of Science (JSPS) Grant-in-Aid for Scientific Research (C) (26430108), Grant-in-Aid for Scientific Research on Innovative Areas (15H01482).

CONFLICT OF INTEREST

The authors declare no conflict of interest.

REFERENCES

Abdelhaleem M (2004a) Over-expression of RNA helicases in cancer. *Anticancer Res* **24**(6): 3951–3953.

Abdelhaleem M, Maltais L, Wain H (2003) The human DDX and DHX gene families of putative RNA helicases. *Genomics* **81**(6): 618–622.

Abdelhaleem M (2004b) Do human RNA helicases have a role in cancer? *Biochim Biophys Acta* **1704**(1): 37–46.

Bady P, Diserens AC, Castella V, Kalt S, Heinimann K, Hamou MF, Delorenzi M, Hegi ME (2012) DNA fingerprinting of glioma cell lines and considerations on similarity measurements. *Neuro Oncol* **14**(6): 701–711.

Bhat KP, Balasubramaniyan V, Vaillant B, Ezhilarasan R, Hummelink K, Hollingsworth F, Wani K, Heathcock L, James JD, Goodman LD, Conroy S, Long L, Lelic N, Wang S, Gumin J, Raj D, Kodama Y, Raghunathan A, Olar A, Joshi K, Pelloski CE, Heimberger A, Kim SH, Cahill DP, Rao G, Den Dunnen WF, Boddeke HW, Phillips HS, Nakano I, Lang FF, Colman H, Sulman EP, Aldape K (2013) Mesenchymal Differentiation Mediated by NF-κB Promotes Radiation Resistance in Glioblastoma. *Cancer Cell* **24**(3): 331–346.

Bol GM, Xie M, Raman V (2015) DDX3, a potential target for cancer treatment. *Mol Cancer* **14**: 188.

Bourgeois CF, Mortreux F, Auboeuf D (2016) The multiple functions of RNA helicases as drivers and regulators of gene expression. *Nat Rev Mol Cell Biol* **17**(7): 426–438.

Brennan CW, Verhaak RG, McKenna A, Campos B, Noushmehr H, Salama SR, Zheng S, Chakravarty D, Sanborn JZ, Berman SH, Beroukhim R, Bernard B, Wu CJ, Genovese G, Shmulevich I, Barnholtz-Sloan J, Zou L, Vegesna R, Shukla SA, Ciriello G, Yung WK, Zhang W, Sougnez C, Mikkelsen T, Aldape K, Bigner DD, Van Meir EG, Prados M, Sloan A, Black KL, Eschbacher J, Finocchiaro G, Friedman W, Andrews DW, Guha A, Iacocca M, O'Neill BP, Foltz G, Myers J, Weisenberger DJ, Penny R, Kucherlapati R, Perou CM, Hayes DN, Gibbs R, Marra M, Mills GB, Lander E, Spellman P, Wilson R, Sander C, Weinstein J, Meyerson M, Gabriel S, Laird PW, Haussler D, Getz G, Chin L. TCGA Research Network (2013) The somatic genomic landscape of glioblastoma. *Cell* **155**(2): 462–477.

Chao CH, Chen CM, Cheng PL, Shih JW, Tsou AP, Lee YH (2006) DDX3, a DEAD box RNA helicase with tumor growth-suppressive property and transcriptional regulation activity of the p21waf1/cip1 promoter, is a candidate tumor suppressor. *Cancer Res* **66**(13): 6579–6588.

Chen HH, Yu HI, Cho WC, Tarn WY (2015) DDX3 modulates cell adhesion and motility and cancer cell metastasis via Rac1-mediated signaling pathway. *Oncogene* **34**(21): 2790–2800.

Copeland NG, Jenkins NA (2010) Harnessing transposons for cancer gene discovery. *Nat Rev Cancer* **10**(10): 696–706.

DeNicola GM, Karreth FA, Adams DJ, Wong CC (2015) The utility of transposon mutagenesis for cancer studies in the era of genome editing. *Genome Biol* **16**: 229.

Faber ZJ, Chen X, Gedman AL, Boggs K, Cheng J, Ma J, Radtke I, Chao JR, Walsh MP, Song G, Andersson AK, Dang J, Dong L, Liu Y, Huether R, Cai Z, Mulder H, Wu G, Edmonson M, Rusch M, Qu C, Li Y, Vadodaria B, Wang J, Hedlund E, Cao X, Yergeau D, Nakitandwe J, Pounds SB, Shurtleff S, Fulton RS, Fulton LL, Easton J, Parganas E, Pui CH, Rubnitz JE, Ding L, Mardis ER, Wilson RK, Gruber TA, Mullighan CG, Schlenk RF, Paschka P, Döhner K, Döhner H, Bullinger L, Zhang J, Klco JM, Downing JR (2016) The genomic landscape of core-binding factor acute myeloid leukemias. *Nat Genet* **48**(12): 1551–1556.

Fourmann JB, Schmitzová J, Christian H, Urlaub H, Ficner R, Boon KL, Fabrizio P, Lührmann R (2013) Dissection of the factor requirements for spliceosome disassembly and the elucidation of its dissociation products using a purified splicing system. *Genes Dev* **27**(4): 413–428.

Fuller-Pace FV (2006) DExD/H box RNA helicases: multifunctional proteins with important roles in transcriptional regulation. *Nucleic Acids Res* **34**(15): 4206–4215.

Ikushima H, Todo T, Ino Y, Takahashi M, Miyazawa K, Miyazono K (2009) Autocrine TGF-beta signaling maintains tumourigenicity of glioma-initiating cells through Sry-related HMG-box factors. *Cell Stem Cell* **5**(5): 504–514.

Jiang ZH, Wu JY (1999) Alternative splicing and programmed cell death. *Proc Soc Exp Biol Med* **220**(2): 64–72.

Koodathingal P, Novak T, Piccirilli JA, Staley JP (2010) The DEAH box ATPases Prp16 and Prp43 cooperate to proofread 5' splice site cleavage during pre-mRNA splicing. *Mol Cell* **39**(3): 385–395.

Korkolopoulou P, Levidou G, Saetta AA, El-Habr E, Eftichiadis C, Demenagas P (2008) Expression of nuclear factor-kappaB in human astrocytomas: relation to pI kappa Ba, vascular endothelial growth factor, Cox-2, microvascular characteristics, and survival. *Hum Pathol* **39**: 1143–1152.

Koso H, Takeda H, Yew CC, Ward JM, Nariai N, Ueno K, Nagasaki M, Watanabe S, Rust AG, Adams DJ, Copeland NG, Jenkins NA (2012) Transposon mutagenesis identifies genes that transform neural stem cells into glioma-initiating cells. *Proc Natl Acad Sci USA* **109**(44): 2998–3007.

Koso H, Yi H, Sheridan P, Miyano S, Ino Y, Todo T, Watanabe S (2016) Identification of RNA-binding protein LARP4B as a tumor suppressor in glioma. *Cancer Res* **76**(8): 2254–2264.

Lai MC, Lee YH, Tarn WY (2008) The DEAD-box RNA helicase DDX3 associates with export messenger ribonucleoproteins as well as tip-associated protein and participates in translational control. *Mol Biol Cell* **19**(9): 3847–3858.

Levin VA, Leibel SA, Gutin PH (2001) Neoplasms of the central nervous system. In: DeVita VT, Jr., Hellman S, Rosenberg SA (eds). *Cancer: Principles and Practice of Oncology*. (6th edn). Lippincott Williams & Wilkins: Philadelphia, PA, USA, pp 2100–2160.

Lu H, Lu N, Weng L, Yuan B, Liu YJ, Zhang Z (2014) DHX15 senses double-stranded RNA in myeloid dendritic cells. *J Immunol* **193**(3): 1364–1372.

Marta I, Marek K (2015) NF-κB and IRF pathways: cross-regulation on target genes promoter level. *BMC Genomics* **16**: 307.

Mosallanejad K, Sekine Y, Ishikura-Kinoshita S, Kumagai K, Nagano T, Matsuzawa A, Takeda K, Naguro I, Ichijo H (2014) The DEAH-box RNA helicase DHX15 activates NF-κB and MAPK signaling downstream of MAVS during antiviral responses. *Sci Signal* **7**(323): ra40.

Niu Z, Jin W, Zhang L, Li X (2012) Tumor suppressor RBM5 directly interacts with the DExD/H-box protein DHX15 and stimulates its helicase activity. *FEBS Lett* **586**(7): 977–983.

Patel SS, Donmez I (2006) Mechanisms of helicases. *J Biol Chem* **281**(27): 18265–18268.

Robert F, Pelletier J (2013) Perturbations of RNA helicases in cancer. *Wiley Interdiscip Rev RNA* **4**(4): 333–349.

Soto-Rifo R, Rubilar PS, Limousin T, de Breyne S, Décimo D, Ohlmann T (2012) DEAD-box protein DDX3 associates with eIF4F to promote translation of selected mRNAs. *EMBO J* **31**(18): 3745–3756.

Steimer L, Klostermeier D (2012) RNA helicases in infection and disease. *RNA Biol* **9**(6): 751–771.

Suthar MK, Purva M, Maherchandani S, Kashyap SK (2016) Identification and in silico analysis of cattle DExH/D box RNA helicases. *Springerplus* **5**: 25.

Svitkin YV, Pause A, Haghighat A, Pyronnet S, Witherell G, Belsham GJ, Sonenberg N (2001) The requirement for eukaryotic initiation factor 4A (elF4A) in translation is in direct proportion to the degree of mRNA 5' secondary structure. *RNA* **7**(3): 382–394.

Tanner NK, Cordin O, Banroques J, Doére M, Linder P (2003) The Q motif: a newly identified motif in DEAD box helicases may regulate ATP binding and hydrolysis. *Mol Cell* **11**(1): 127–138.

Tuteja N, Tuteja R (2004a) Prokaryotic and eukaryotic DNA helicases. Essential molecular motor proteins for cellular machinery. *Eur J Biochem* **271**(10): 1835–1848.

Tuteja N, Tuteja R (2004b) Unraveling DNA helicases. Motif, structure, mechanism and function. *Eur J Biochem* **271**(10): 1849–1863.

Tuteja N, Tuteja R (2006) DNA helicases as molecular motors: an insight. *Physica Acta* **372**: 70–83.

Umate P, Tuteja N, Tuteja R (2011) Genome-wide comprehensive analysis of human helicases. *Commun Integr Biol* **4**(1): 118–137.

Walid MS (2008) Prognostic factors for long-term survival after glioblastoma. *Perm J* **12**(4): 45–48.

Wang P, Zhu S, Yang L, Cui S, Pan W, Jackson R, Zheng Y, Rongvaux A, Sun Q, Yang G, Gao S, Lin R, You F, Flavell R, Fikrig E (2015) Nlrp6 regulates intestinal antiviral innate immunity. *Science* **350**(6262): 826–830.

Workman P, Aboagye EO, Balkwill F, Balmain A, Bruder G, Chaplin DJ, Double JA, Everitt J, Farningham DA, Glennie MJ, Kelland LR, Robinson V, Stratford IJ, Tozer GM, Watson S, Wedge SR, Eccles SA. Committee of the National Cancer Research Institute (2010) Guidelines for the welfare and use of animals in cancer research. *Br J Cancer* **102**(11): 1555–1577.

Zhang R, Banik NL, Ray SK (2007) Combination of all-trans retinoic acid and interferon-gamma suppressed PI3K/Akt survival pathway in glioblastoma T98G cells whereas NF-kappaB survival signaling in glioblastoma U87MG cells for induction of apoptosis. *Neurochem Res* **32**(12): 2194–2202.

Supplementary Information accompanies this paper on British Journal of Cancer website (http://www.nature.com/bjc)